



# Atmospheric pressure MOCVD growth of high-quality ZnO films on GaN/Al<sub>2</sub>O<sub>3</sub> templates

Jiangnan Dai, Hechu Liu, Wenqing Fang, Li Wang, Yong Pu, Yufeng Chen, Fengyi Jiang\*

*Education Ministry Research Center for Luminescence Materials and Devices, Nanchang University, 235 East Nanjing Road, Nanchang 330047, PR China*

Received 28 October 2004; received in revised form 28 April 2005; accepted 13 May 2005

Available online 11 July 2005

Communicated by R. James

## Abstract

In this paper, we present the epitaxial growth of high-quality ZnO thin films on GaN/c-Al<sub>2</sub>O<sub>3</sub> templates by atmospheric pressure metal organic chemical vapor deposition (MOCVD) using deionized water (H<sub>2</sub>O) and diethyl zinc (DEZn) as the O and Zn sources, respectively. Surface morphology of the films studied by metal-phase interference microscopy and AFM showed that the growth of the ZnO films followed the regular hexagonal columnar structure with about 19 μm grain diameter. High-resolution X-ray double-crystal diffraction was used to investigate the structural properties of the as-grown films. The FWHMs of the (0002) and (10 $\bar{1}$ 2)  $\omega$ -rocking curves were 182 and 358 arcsec, respectively, indicating the small mosaicity and low dislocation density of the films. The optical properties of the films were investigated by room temperature photoluminescence and temperature-dependent PL spectra. Free excitons X<sub>A</sub> and the  $n = 2$  state of FX<sub>A</sub> can be clearly observed at 3.375 and 3.419 eV at 10 K, respectively. The domination of the free exciton and the appearance of its four replicas strongly indicate the high quality of the film.

© 2005 Elsevier B.V. All rights reserved.

PACS: 75.55.C; 87.64.Bx; 78.55.-m

Keywords: A1. AFM; A1. Photoluminescence; A1. X-ray diffraction; A3. MOCVD; B2. ZnO/GaN/Al<sub>2</sub>O<sub>3</sub>

## 1. Introduction

Due to its wide gap of 3.37 eV and its ultraviolet lasing at room temperature (RT) [1] and its large

exciton binding energy of 60 meV [2], ZnO has many potential applications in short wavelength light-emitting devices, such as UV and blue LED/LDs. Many growth techniques for single-crystalline ZnO films have been studied, such as molecular beam epitaxy [3], metalorganic chemical vapor deposition (MOCVD) [4], RF magnetron

\*Corresponding author. Tel.: +86 791 8305673.

E-mail address: [Jiangfy@vip.163.com](mailto:Jiangfy@vip.163.com) (F.-Y. Jiang).

sputtering [5], and pulsed laser deposition [6]. Among these techniques, MOCVD has many advantages for bulk production and has been proven to be suitable for growth of many electronic and optoelectronic materials. In addition, investigations revealed that atmospheric pressure growth of GaN films usually yield larger grain size and higher mobility than low-pressure growth [7–9]. So AP-MOCVD will be a possible way to improve the crystalline quality of ZnO film. Many growths of ZnO films grown by LP-MOCVD have been reported, but only a few investigations on AP-MOCVD growth of high-quality ZnO films have been reported [10–13].

Recently, there has been great progress in the growth of ZnO thin films. But applicable ZnO optoelectronic devices have not yet been fabricated, mainly because sufficiently effective p-type ZnO thin films have not been obtained till now. To solve the p-type doping problems, it is necessary to grow higher-quality ZnO thin films. One of the key issues to grow high-quality ZnO thin films is to find a lattice-matched substrate. Although ZnO bulk crystal can be obtained now, it is very expensive and its size is small. Therefore, heteroepitaxy is still the most used method. GaN ( $a = 3.189 \text{ \AA}$ ,  $c = 5.185 \text{ \AA}$ ) and ZnO ( $a = 3.2498 \text{ \AA}$ ,  $c = 5.2066 \text{ \AA}$ ) [14] have close lattice constants (the mismatch is less than 2%) and a small difference between the in-plane linear thermal expansion coefficients ( $\alpha_{\text{GaN}} = 5.59 \times 10^{-6}$  and  $\alpha_{\text{ZnO}} = 6.51 \times 10^{-6} \text{ K}^{-1}$ ) [15], so GaN is possibly a suitable substrate for the growth of ZnO epitaxial layers. At present, due to the lack of low-cost GaN bulk crystal and the availability of a technique of growing high-quality GaN films on  $\text{Al}_2\text{O}_3$  substrate, it is a feasible method to use the GaN epilayer as the buffer layers on other substrates for the growth of ZnO epitaxial layers. Since Vispute et al. [16] first reported the growth of ZnO films on epi-GaN/sapphire (0001) by PLD, there have been a few reports on the growth of ZnO films using the GaN epilayer as the buffer layers on other substrates by RF magnetron sputtering [17], MBE [18] and MOVPE [19].

In this paper, we report the epitaxial growth of high-quality ZnO thin film on epi-GaN /c- $\text{Al}_2\text{O}_3$

templates by atmospheric pressure metalorganic chemical vapor deposition.

## 2. Experimental procedure

ZnO thin films were deposited by a home-built vertical atmospheric pressure MOCVD system with a rotating disk reactor (see Fig. 1). We have reported the epitaxial growth of ZnO thin films on c- $\text{Al}_2\text{O}_3$  (0001) substrates by our home-built vertical atmospheric pressure MOCVD system [20]. The MOCVD growth of GaN/ $\text{Al}_2\text{O}_3$  templates on 2 in. c- $\text{Al}_2\text{O}_3$  (0001) substrates was performed in a Thomas Swan close-coupled showerhead (CCS) MOCVD reactor system. During the growth, trimethyl gallium (TMGa) and ammonia ( $\text{NH}_3$ ) were used as the source materials of Ga and N, respectively. The thickness of the GaN layer was about  $2 \mu\text{m}$ . These structures were transferred into our rotating disk vertical reactor of AP-MOCVD without the preliminary cleaning and polishing procedures. We used deionized water ( $\text{H}_2\text{O}$ ) ( $\rho = 18.2 \text{ M}\Omega\text{cm}$ ) and 6N-purity DEZn as the O and Zn sources, respectively, and 7N-purity nitrogen as the carrier gas. Before growth, the GaN/ $\text{Al}_2\text{O}_3$  templates were thermally cleaned at  $850 \text{ }^\circ\text{C}$  for 20 min. Typical growth conditions were as follows: the reactor-chamber pressure was 760 Torr. A two-step growth process was adopted. In the first step, a  $150 \text{ \AA}$  ZnO buffer layer was grown at  $200 \text{ }^\circ\text{C}$  using DEZn and  $\text{H}_2\text{O}$  at flow rates of  $813 \mu\text{mol/min}$  and  $0.039 \text{ mol/min}$ , respectively. Then the buffer layer was processed

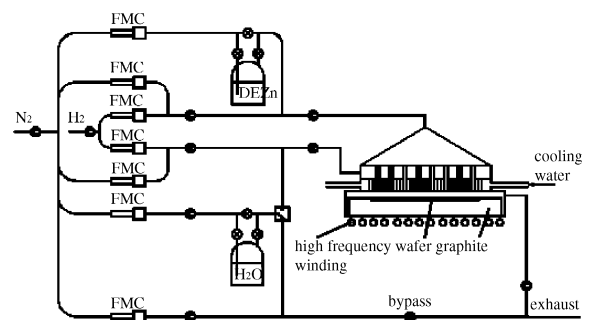


Fig. 1. Schematic sketch of the AP-MOCVD system for growth of ZnO.

at 800 °C for 5 min for re-crystallization. In the second step, the main ZnO epitaxial layer was deposited under the growth temperature of 680 °C using DEZn and H<sub>2</sub>O at flow rates of 0.011 and 0.183 mol/min, respectively. The total carrier gas flow rate was about 15 000 sccm. The growth rate of the main ZnO layer was 4 μm/h, resulting in the total thickness of 2 μm. For comparative analysis, a ZnO film grown directly on a c-Al<sub>2</sub>O<sub>3</sub> (0001) substrate under the same conditions was also prepared.

The microscopic image of the ZnO film was observed by metal-phase interference microscopy (OLYMPUS, BX51). Surface morphology of the ZnO layers was studied by atomic force microscopy (AFM) in a contact mode using a Chinese Benyuan Nano Instrument 3100 system. Crystal perfection of the samples was examined by high-resolution double-crystal X-ray diffractometry (HRXRD) (QC200, BEDE Instruments, UK). The Cu K<sub>α</sub> line ( $\lambda = 1.54056 \text{ \AA}$ ) was used as the source, and Ge (004) was used as the monochromator. Photoluminescence (PL) of the film was measured under RT and at 10 K using the 325 nm line of a He–Cd laser (8 mW) as the excitation source.

### 3. Results and discussion

The as-grown films were transparent and have mirror-like surfaces. Fig. 2 shows the microscopic image of a typical ZnO film at  $\times 200$  magnification by metal-phase interference microscopy. The average grain diameter of the film was about 18 μm. We observed many regular hexagonal grain particles in the microscopic image. It proved that the regular hexagonal column growth of the ZnO film strictly followed the hexagonal structure of the GaN epilayer. Fig. 3 shows the AFM image of a typical sample for a scan area of 25 μm  $\times$  25 μm. Hexagonal-like growths can be clearly seen on the surface. The grain diameter of the film was about 19 μm, much larger than reported grain size for a ZnO film deposited by MBE [21], PLD [22] and LP-MOCVD [23]. The root mean square (RMS) roughness as determined by AFM (25 μm  $\times$  25 μm) of the film surface was about 4.5 nm. The mechan-

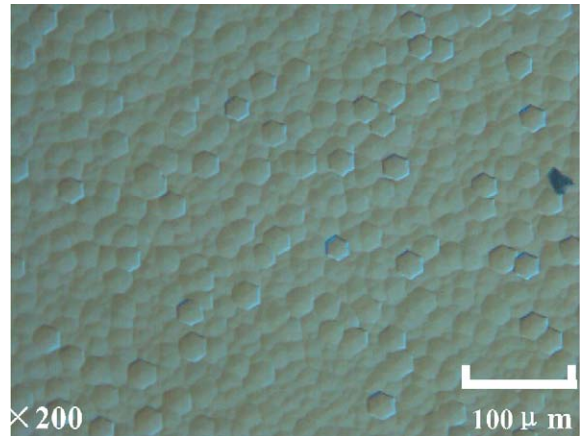


Fig. 2. Interference Micrograph of the surface of ZnO/GaN/Al<sub>2</sub>O<sub>3</sub> film.

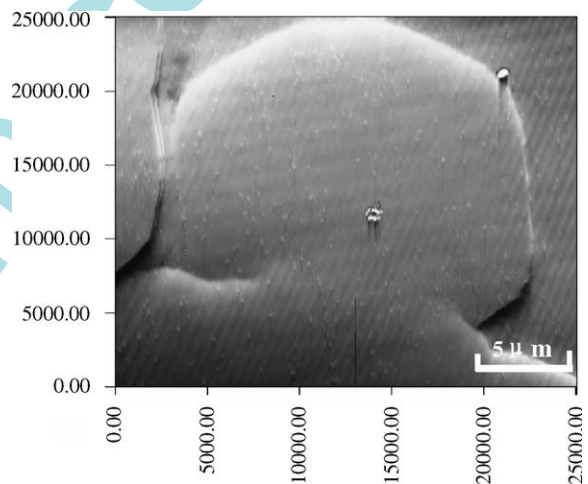


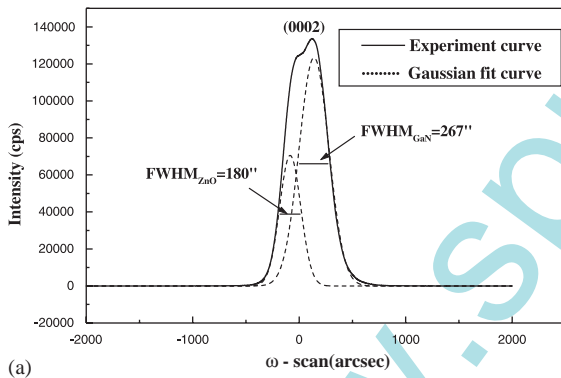
Fig. 3. AFM image of ZnO/GaN/Al<sub>2</sub>O<sub>3</sub> film (25 μm  $\times$  25 μm).

ism for the formation of large grain size by AP-MOCVD has been studied by several investigations [7,8]. It is believed that the nucleation density on the substrate for AP growth is less than that for low-pressure growth. So for AP-MOCVD, the lateral growth for nucleation will proceed a long time before they coalesce, thus forming large grains.

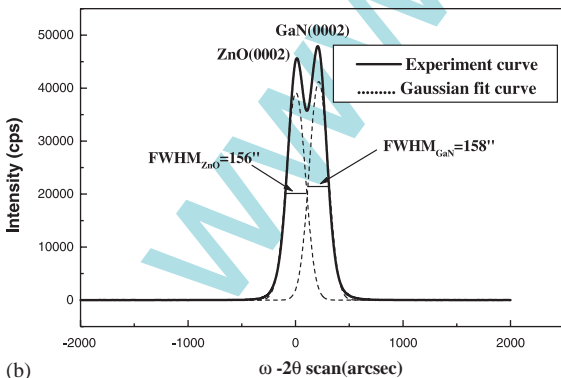
It is well known that the X-ray diffraction is complementary to the transmission electron microscopy (TEM) and etch pit densities (EPD)

methods, because it is non-destructive and can be used to determine dislocation densities. The rocking curve full-width at half-maximum (FWHM) value is taken as a figure of merit for crystalline perfection. Heying et al. [24] have reported that the (0002) rocking curve is sensitive only to the screw or mixed dislocations, while the skew (10 $\bar{1}2$ ) rocking curve is sensitive to all the dislocations content in the GaN films. Thus, the broadening of the skew (10 $\bar{1}2$ ) unsymmetrical rocking curve is a more reliable indicator of structural quality. In our experiments, FWHMs of (0002) and skew (10 $\bar{1}2$ )  $\omega$ -rocking curves were used as the indicators of screw and all the dislocations, respectively. Fig. 4(a) shows the symmetric (0002)  $\omega$ -rocking curve of a typical sample of ZnO/GaN/Al<sub>2</sub>O<sub>3</sub> films. The symmetry of the  $\omega$ -rocking curve implied that the ZnO peak was overlapped by the GaN peak because their lattice constants are

very close to each other. By Gaussian fit, we obtained a FWHM of 182arcsec for the ZnO (0002)  $\omega$ -rocking curve, which is even smaller than the FWHM value (267arcsec) of GaN in GaN/Al<sub>2</sub>O<sub>3</sub> template. Fig. 4(b) shows the (0002)  $\omega$ -2 $\theta$  diffraction profile of the sample. By Gaussian fit, the FWHM values for the ZnO and GaN layers are 156 and 158 arcsec, respectively. Fig. 5 shows the skew (10 $\bar{1}2$ )  $\omega$ -rocking curve of a ZnO epilayer and an epi-GaN substrate. The FWHM values of the ZnO and epi-GaN layer are 358 and 320 arcsec, respectively. Heying et al. [24] have reported that the GaN sample with a (102) FWHM of 413arcsec has a total threading dislocation density of  $4 \times 10^8 \text{ cm}^{-2}$ , so we estimate that the dislocation density of our ZnO sample is less than or in the range of  $10^8 \text{ cm}^{-2}$ . Table 1 shows the FWHM values of (0002) and skew-(10 $\bar{1}2$ ) XRC in ZnO on GaN template, ZnO on c-Al<sub>2</sub>O<sub>3</sub> grown at the same condition and device-grade GaN on c-Al<sub>2</sub>O<sub>3</sub> grown by MOCVD. Such narrow FWHM values of ZnO films on GaN templates suggest that there were fewer threading dislocations in ZnO films on GaN templates than in ZnO films directly on c-Al<sub>2</sub>O<sub>3</sub> (0001) substrate. Moreover, these values of ZnO films on GaN templates were narrower than those of this device-grade GaN specimen which was 2 $\mu\text{m}$  thick GaN grown on c-Al<sub>2</sub>O<sub>3</sub> (0001) substrate by a Thomas Swan MOCVD system in our laboratory.



(a)



(b)

Fig. 4. The (0002) scan curves of ZnO/GaN/Al<sub>2</sub>O<sub>3</sub> film: (a)  $\omega$ -scan; (b)  $\omega$ -2 $\theta$  scan.

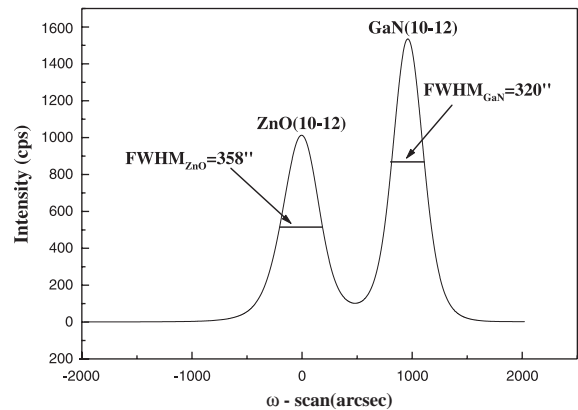
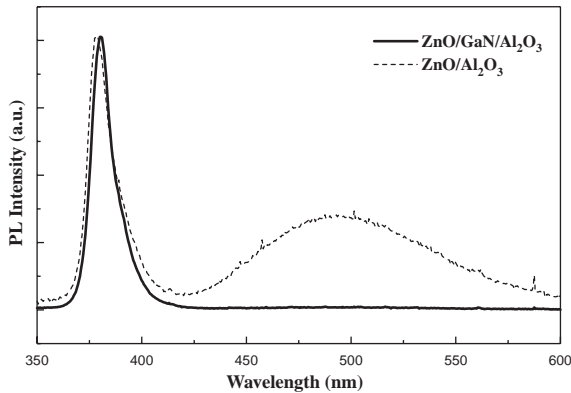
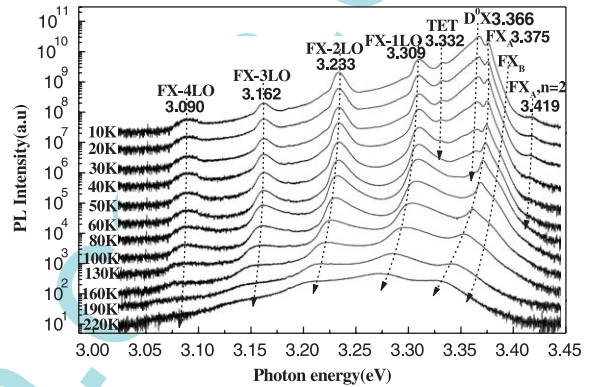


Fig. 5. The (10 $\bar{1}2$ )  $\omega$ -rocking curve of ZnO/GaN/Al<sub>2</sub>O<sub>3</sub> film.

Table 1

FWHMs of XRD measurements in different geometries of ZnO films on various substrates and of device-grade GaN films on sapphire

Epilayer/substrate	FWHM (0002) $\omega$ -scans (arcsec)	FWHM (0002) $\omega$ -2 $\theta$ scans (arcsec)	FWHM (10 $\bar{1}$ 2) $\omega$ -scans (arcsec)
ZnO/GaN/c-Al <sub>2</sub> O <sub>3</sub>	182	156	358
ZnO/c-Al <sub>2</sub> O <sub>3</sub>	386	295	650
GaN/c-Al <sub>2</sub> O <sub>3</sub>	365	238	410

Fig. 6. Room temperature PL spectra of ZnO/GaN/Al<sub>2</sub>O<sub>3</sub> film and ZnO/Al<sub>2</sub>O<sub>3</sub> film.Fig. 7. Temperature-dependent PL spectra of ZnO/GaN/Al<sub>2</sub>O<sub>3</sub> film from 10 K to 220 K.

PL spectra for ZnO/GaN/Al<sub>2</sub>O<sub>3</sub> and ZnO/Al<sub>2</sub>O<sub>3</sub> films carried out at RT are shown in Fig. 6. Strong ultraviolet (UV) emission coming from exciton emission could be observed in both samples. However, deep-level emission at 500 nm was observed in ZnO/Al<sub>2</sub>O<sub>3</sub> film. The deep-level emission, which is usually defect-related, was difficult to observe in our ZnO/GaN/Al<sub>2</sub>O<sub>3</sub> sample. To further study the optical properties of the film, low-temperature PL measurements at 10 K and temperature-dependent PL experiments of ZnO/GaN/Al<sub>2</sub>O<sub>3</sub> film from 10 K to 220 K were performed.

Fig. 7 shows temperature-dependent PL spectra of ZnO/GaN/Al<sub>2</sub>O<sub>3</sub> film from 10 K to 220 K. From the low-temperature PL spectrum of the ZnO/GaN/Al<sub>2</sub>O<sub>3</sub> film collected at 10 K, we see that the energy position of the dominant peak is 3.366 eV. It can be ascribed to the exciton transition bounded to neutral donors (D<sup>0</sup>X), since a similar peak has been observed at 3.367 eV for

ZnO films on epi-GaN/Al<sub>2</sub>O<sub>3</sub> grown by MBE [25]. Another peak at 3.332 eV originates from two electron transitions (TET) [26], because the luminescence line disappears together with the BE lines with increasing temperature. The emission line at 3.375 eV can be assigned to the free exciton X<sub>A</sub> (FX<sub>A</sub>), and that at 3.419 eV to the  $n = 2$  state of FX<sub>A</sub> [27]. Although the  $n = 2$  state of FX<sub>A</sub> has been observed in high-quality ZnO bulk crystals [28,29] and homoepitaxial ZnO films [30], it has not been observed in heteroepitaxial ZnO films. The low-energy tail extending from the excitonic emission peaks due to the lattice deformation is much reduced, which allows the observation of the phonon replicas of the free excitons [31]. The presence of free excitons at low temperature offers evidence of the high purity and crystal quality of the ZnO epilayer. The peaks at 3.090, 3.162, 3.233 and 3.309 eV should be attributed to 1LO, 2LO, 3LO and 4LO phonon replicas of the free exciton, since these lines remain up to 220 K together with

the zero phonon line of  $FX_A$ . It should be noted that the energy difference between the zero phonon line and 1LO phonon replica line (66 meV) is somewhat smaller than the energy of a LO phonon (72 meV) calculated by Klingshirn [32], although the difference between 1LO phonon replica line and 2LO phonon replica line (76 meV) almost coincides with the theoretical value. In addition, from the temperature-dependent PL spectra of ZnO/GaN/Al<sub>2</sub>O<sub>3</sub> film from 10 K to 220 K, we see that as the temperature increased from 10 to 80 K, the intensities of free excitons  $X_A$  transition at 3.375 eV observed at 10 K increased, while those of the bound exciton peaks at 3.366 eV decreased. The bound exciton peaks disappeared above 100 K, and only the  $FX_A$  and  $FX_B$  peaks and phonon replicas of the free exciton were observed. The domination of free exciton and the appearance of its four phonon replicas strongly indicate the high quality of the film.

#### 4. Conclusion

In conclusion, we fabricated high quality ZnO epitaxial films with atmospheric pressure MOCVD on GaN/Al<sub>2</sub>O<sub>3</sub> templates. With a growth rate of typically 4  $\mu\text{m}/\text{h}$  at a growth temperature of 680 °C and a pressure of 760 Torr, the regular hexagonal column growth mode was observed by metal-phase interference microscopy and AFM. The X-ray diffraction investigations showed a single crystallinity, a wurtzite phase with a FWHM of (0002), an  $\omega$ -scan curve of 182 arcsec and a (0002)  $\omega$ -2 $\theta$  scan curve of 156 arcsec. The FWHM value of skew (10 $\bar{1}$ 2)  $\omega$ -scan curve of 358 arcsec showed that the threading dislocation density of the ZnO films was less than or on the order of  $10^8 \text{ cm}^{-2}$ , which is comparable to device-level GaN films. The ZnO/GaN/Al<sub>2</sub>O<sub>3</sub> film showed very sharp near-band-edge luminescence at RT. The absence of the deep-level emission peak indicates that the ZnO films are of excellent optical quality and have few interior defects. Compared with the ZnO/Al<sub>2</sub>O<sub>3</sub> film grown at the same conditions, the ZnO/GaN/Al<sub>2</sub>O<sub>3</sub> film showed better crystalline and optical quality. From the low temperature PL spectra of ZnO thin films grown on GaN/Al<sub>2</sub>O<sub>3</sub>

templates, the  $FX_A$  and  $D^0X$  emissions and the  $n = 2$  state of  $FX_A$  were clearly observed at 10 K, indicating high optical quality of the films. The high morphological, crystalline and optical quality of ZnO films opens broad prospects for device applications.

#### Acknowledgements

The authors would like to thank Prof. Zikang Tang for supplying assistance with the PL spectrum analysis. This work was supported by 863-project with contract no. 2003AA302160 and the Electronic Development Fund of Information Industry in China.

#### References

- [1] Z.K. Tang, G.K.L. Wong, P. Yu, Appl. Phys. Lett. 72 (1998) 3270.
- [2] W.Y. Liang, A.D. Yoffe, Phys. Rev. Lett. 20 (1968) 59.
- [3] P. Fons, K. Iwata, S. Niki, A. Yamada, K. Matsubara, J. Crystal Growth 201 (1999) 627.
- [4] Y. Kashiwaba, F. Katahira, K. Haga, T. Sekiguchi, H. Watanabe, J. Crystal Growth 221 (2000) 431.
- [5] A. Nahhas, H.K. Kim, Appl. Phys. Lett. 78 (11) (2001) 1511.
- [6] Y.R. Ryu, J.M. Wrobel, H.M. Jeong, P.F. Miceli, H.W. White, J. Crystal Growth 216 (2000) 326.
- [7] D.D. Koleske, A.E. Wickenden, R.L. Henry, M.E. Twigg, J.C. Culbertson, Appl. Phys. Lett. 73 (1998) 2019.
- [8] F.A. Ponce, MRS Bulletin 22 (1997) 51.
- [9] S. Einfeldt, T. Bottecher, S. Figge, D. Hommel, J. Crystal Growth 230 (2001) 357.
- [10] Y. Kashiwaba, F. Katahira, K. Haga, T. Sekiguchi, H. Watanabe, J. Crystal Growth 221 (2000) 431.
- [11] S. Bethke, H. Pan, B.W. Wessels, Appl. Phys. Lett. 52 (1988) 138.
- [12] B.P. Zhang, Y. Segawa, K. Wakatsuki, Y. Kashiwaba, Appl. Phys. Lett. 79 (2001) 3953.
- [13] C.R. Gorla, N.W. Emanetoglu, S. Liang, W.E. Mayo, Y. Lu, J. Appl. Phys. 85 (1999) 2595.
- [14] International Center for Diffraction Data, PDF-2 card 36–1451.
- [15] B.M. Ataev, W.V. Lundin, V.V. Mamedov, et al., J. Phys.: Condens. Matter 13 (2001) L211.
- [16] R.D. Vispute, V. Talyansky, S. Choopun, et al., Appl. Phys. Lett. 73 (1998) 348.
- [17] A. Nahhas, H.K. Kima, J. Blachere Appl. Phys. Lett. 78 (2001) 1511.
- [18] N. Izyumskaya, V. Avrutin, W. Schoch, et al., J. Crystal Growth 269 (2004) 356.

- [19] A. Dadgar, N. Oleynik, D. Forster, et al., *J. Crystal Growth* 267 (2004) 140.
- [20] Y. Chen, F. Jiang, L. Wang, et al., *J. Crystal Growth* 268 (2004) 71.
- [21] T. Matsumoto, H. Kato, K. Miyamoto, M. Sano, *Appl. Phys. Lett.* 81 (2002) 1231.
- [22] E.M. Kaidashev, M. Lorenz, H. von Wenckstem, A. Rahm, H.-C. Semmelhack, *Appl. Phys. Lett.* 82 (2003) 3091.
- [23] N. Oleynik, A. Dadgar, J. Christen, J. Blasing, M. Adam, *Phys. Stat. Sol. (a)* 192 (2002) 189.
- [24] B. Heying, X.H. Wu, S. Keller, et al., *Appl. Phys. Lett.* 68 (1996) 643.
- [25] H.J. Ko, Y.F. Chen, T. Yao, et al., *Appl. Phys. Lett.* 77 (2000) 537.
- [26] S.W. Jung, W.I. Park, H.D. Cheong, et al., *Appl. Phys. Lett.* 80 (2002) 1924.
- [27] D.G. Thomas, *J. Phys. Chem. Solids* 15 (1960) 86.
- [28] D.C. Reynolds, D.C. Look, B. Jogai, C.W. Litton, G. Cantwell, W.C. Harsch, *Phys. Rev. B* 60 (1999) 2340.
- [29] M. Suscavage, M. Harris, D. Bliss, P. Yip, S.-Q. Wang, D. Schewall, L. Bouthillette, J. Baily, M. Callahan, D.C. Look, D.C. Reynolds, R.L. Jones, C.W. Litton, *MRS Internet J. Nitride Semicond. Res* 4S1 G3 (1999) 40.
- [30] H. Katoa, M. Sanoa, K. Miyamotoa, et al., *J. Crystal Growth* 265 (2004) 375.
- [31] Y. Chen, H.-J. Ko, S.-K. Hong, et al., *Appl. Phys. Lett.* 76 (2000) 559.
- [32] C. Klingshirn, *Phys. Stat. Sol. (B)* 71 (1975) 547.

www.spm.com